







Transcriptional characterization of cocaine withdrawal versus extinction within nucleus accumbens in male rats

Received: 18 March 2024

Accepted: 10 March 2025

Published online: 25 March 2025



Freddyson J. Martínez-Rivera ^{1,2,3}, Leanne M. Holt ^{1,3},
Angélica Minier-Toribio ¹, Molly Estill¹, Szu-Ying Yeh ¹, Solange Tofani¹,
Rita Futamura¹, Caleb J. Browne¹, Philipp Mews¹, Li Shen ¹ & Eric J. Nestler ¹✉

Neurobiological alterations seen in addiction amplify during abstinence and compromise relapse prevention. Cocaine use disorder (CUD) exemplifies this phenomenon in which reward regions such as nucleus accumbens (NAc) undergo withdrawal-associated modifications. While genome-wide transcriptional changes in NAc are linked to specific addiction phases, these have not been examined in a context- and NAc-subregion-specific manner during withdrawal vs. extinction. We used cocaine self-administration in male rats combined with RNA-sequencing of NAc-core and -shell to transcriptionally profile withdrawal in the home-cage, in the previous drug context, or after extinction. As expected, home-cage withdrawal maintained seeking, whereas extinction reduced it. By contrast, withdrawal involving the drug context only increased seeking. Bioinformatic analyses revealed specific gene expression patterns and networks associated with these states. Comparing NAc datasets of CUD patients highlighted conserved transcriptomic signatures with rats experiencing withdrawal in the drug context. Together, this work reveals fundamental mechanisms that can be targeted to attenuate relapse.

Substance use disorder (SUD) is characterized by neurobehavioral adaptations that underlie devastating social, occupational, and health conditions that drive relapse and prevent effective treatment for most people. Remission often fails because withdrawal-associated symptoms become overwhelming and increase the propensity for relapse¹. While extinction-based therapies and adjunct medication have been used to manage withdrawal symptoms², these approaches show limited success, due in part to the lack of understanding of the fundamental molecular mechanisms involved.

Central to SUD-associated adaptations, the nucleus accumbens (NAc) and its two subregions (core and shell) are associated with signaling specific reward-related processes and exhibit orchestrated transcriptional changes in a time-, phase- and context-dependent manner^{3–6}. It is suggested that the NAc-core drives drug-seeking

behaviors, whereas the NAc-shell acts as an integrative hub for saliency and extinction processes⁷. However, to date, the transcriptional changes in the NAc-core and NAc-shell subregions during withdrawal and extinction (WD/Ext) have not yet been characterized in drug self-administration (SA) models.

We used two different withdrawal modalities after chronic cocaine SA in rats⁸, whereby forced abstinence was achieved with repetitive context exposure only (in the absence of drug, levers, or cues) or with home-cage confinement, and compared results during withdrawal to those obtained after full extinction conditions (context/levers/cues). This was combined with genome-wide RNA-sequencing (RNA-seq) of the NAc-core and -shell separately. Bioinformatic analyses were used to reveal gene expression patterns, biological functions, potential upstream regulators, and co-expression modules of

¹Nash Family Department of Neuroscience and Friedman Brain Institute, Icahn School of Medicine at Mount Sinai, New York, USA. ²Present address: Department of Neuroscience, McKnight Brain Institute, College of Medicine, University of Florida, Gainesville, FL, USA. ³These authors contributed equally: Freddyson J. Martínez-Rivera, Leanne M. Holt. ✉e-mail: fmartinezrivera@ufl.edu; leanne.holt@mssm.edu; eric.nestler@mssm.edu

gene networks in an NAc-subregion-specific manner across abstinence conditions. To clinically leverage our transcriptomic findings, we integrated our results with an available transcriptomic dataset of NAc samples from patients with cocaine use disorder (CUD)⁹. Understanding the behavioral and transcriptional correlates of different WD/Ext settings will provide actionable information to better manage relapse triggers and achieve long-term abstinence.

Results

Repeated context exposure in the absence of levers/cues/drug increases drug seeking

To investigate the transcriptional landscape of different forced abstinence scenarios, rats first underwent cocaine SA followed by three different WD/Ext modalities (Fig. 1A). Rats acquired cocaine SA in daily 3-h sessions under an FR1 schedule (0.8 mg/kg/infusion) for 10 days with discrimination observed between active and inactive levers (Fig. 1B; cocaine group: active vs. inactive presses; $F_{(1,92)} = 298.7$, $p < 0.001$). Acquisition was confirmed by comparing cocaine and saline groups (Fig. S1A, B) (Group; $F_{(1,47)} = 94.45$, $p < 0.001$). Two days after the last acquisition session, rats were tested for drug-seeking behavior in a drug-free test (Test 1; T1; Fig. 1C; group \times measurement, $F_{(2, 225)} = 45.07$, $p < 0.001$; within effect, $F_{(2, 225)} = 63.52$, $p < 0.001$, Sidak, cocaine: active vs. inactive; $p < 0.001$; Fig. S1C: saline: active vs. inactive; $p = 0.99$), where cocaine SA rats exhibited elevated seeking compared to their saline counterparts (between effect, $F_{(1, 225)} = 240.8$, $p < 0.001$, Sidak, cocaine vs. saline: active $p < 0.001$, inactive $p = 0.007$, cues $p < 0.001$).

To probe adaptations after WD/Ext paradigms, rats were separated into three subgroups: 1) placement back into the previous drug context (Ctx; context withdrawal), 2) home-cage (HC; home-cage withdrawal), or 3) under full extinction conditions (Ext) (Fig. 1A and D). These groups were matched based on acquisition and T1 (Fig. S1G; acquisition: active, $F_{(2, 44)} = 0.22$, $p > 0.05$; inactive, $F_{(2, 44)} = 3.92$, $p < 0.05$, Sidak, day 1 (only; inset inactive) HC vs. Ext $p < 0.05$; rewards/infusions: $F_{(2, 44)} = 0.40$, $p > 0.05$; T1: $F_{(2, 132)} = 0.63$, $p > 0.05$). Corresponding saline groups (Fig. S1D–F) were also matched (Fig. S1H; acquisition: active, $F_{(2, 27)} = 0.36$, $p > 0.05$; inactive, $F_{(2, 27)} = 1.09$, $p > 0.05$; rewards/infusions: $F_{(2, 27)} = 0.83$, $p > 0.05$; T1: $F_{(2, 81)} = 0.14$, $p > 0.05$).

Two days after the WD/Ext phase, all groups received another drug-seeking test (drug-free; Test 2; T2). As expected, rats receiving full extinction training (context/lever/cues), reduced their seeking (Fig. 1D; active pressing over time: $F_{(5, 183)} = 9.54$, $p < 0.01$; Sidak, first vs. last day of extinction $p = 0.02$). In the absence of acquisition at first, no further extinction occurred in saline conditions (Fig. S1D; time, $F_{(6, 195)} = 2.46$, $p = 0.03$; Sidak, all p 's > 0.05). Both the HC and Ctx groups showed elevated seeking when compared to Ext (Fig. 1E; T2: $F_{(2, 133)} = 54.38$, $p < 0.01$, Sidak, $p < 0.05$), with no differences between HC and Ctx (Fig. 1E, $p > 0.05$, Sidak). Some of these results were observed to a lesser extent in saline Ctx and HC counterparts (Fig. S1E; $F_{(2, 81)} = 12.44$, $p < 0.01$, Sidak, $p < 0.05$). Nonetheless, such effects were dramatically higher in cocaine-exposed groups (Fig. S1I; active; T1: $F_{(1, 71)} = 115.10$, $p < 0.01$; T2: $F_{(1, 71)} = 57.85$, $p < 0.01$, Sidak, $p < 0.01$). Furthermore, when Ext (9.77 ± 1.23) is compared directly against its saline group (3.54 ± 0.87), higher but not significant seeking behavior was still observed (Fig. S1I; active; T2, Sidak, $p > 0.05$), highlighting the impact of previous cocaine SA, where similar effects were also observed in inactive and total presses (Fig. S1I). This was anticipated, given the exploratory behavior of rats, and supports the importance of proper controls.

We compared Test 1 vs. Test 2 in cocaine- or saline-exposed groups. Neither Ctx nor HC demonstrated significant changes in seeking behaviors (active/inactive and cues; Fig. 1F and insets) from T1 to T2 (Fig. 1F; active: group, $F_{(2, 44)} = 10.88$, $p < 0.01$; time, $F_{(1, 44)} = 9.47$, $p < 0.01$, Sidak, $p > 0.05$). In addition, when total lever pressing was analyzed as a potential indicator of generalized seeking behavior in the

absence of the drug (i.e., accompanied by increased inactive lever pressing when contingencies change as observed in similar studies^{10–14}), a higher but not significant increase was observed within the Ctx condition (Fig. 1G, total; T1: 62.5 ± 6.6 ; T2: 73.0 ± 5.8 ; time, $F_{(1, 44)} = 6.64$, $p = 0.01$, Sidak, Ctx T1 vs. Ctx T2: $p = 0.42$), with no differences between Ctx and HC groups, but differing from the Ext group (Fig. 1G; groups, $F_{(2, 44)} = 11.95$, $p < 0.01$, Sidak, T2, Ctx vs. HC: $p = 0.1$, Ctx/HC vs. Ext: $p < 0.01$). Such an effect that was not observed in T1 (Fig. 1G, Sidak, p 's > 0.05) or replicated in saline conditions (Fig. S1J; T1: $F_{(2, 27)} = 0.03$, $p > 0.05$; T2: $F_{(2, 27)} = 5.3$, $p < 0.05$, Sidak, Ctx vs. HC: $p = 0.85$, Ctx vs. Ext: $p = 0.02$, HC vs. Ext: $p = 0.06$). As expected, Ext reduced the animals' seeking from T1 to T2 (Fig. 1F; active: time, $F_{(1, 44)} = 9.47$, $p < 0.01$, Sidak, $p < 0.01$; and insets. Figure 1G; total: time, $F_{(2, 44)} = 11.95$, $p < 0.01$, Sidak, $p < 0.01$). These effects were not recapitulated in saline groups (Fig. S1F and insets), except for Ctx saline. However, cocaine groups still showed higher seeking behavior compared to saline (Fig. S1I; active, inactive and total presses), despite presses for cue light presentation after a long omission break (Fig. S1I–J). This again underscores the importance of appropriate controls, as the withdrawal-associated seeking is impacted both by contexts (as seen under saline conditions) and by drugs.

Subsequent analysis demonstrated subtle but important differences in the distribution of seeking behavior for each cocaine WD/Ext group. Unsurprisingly, Ext demonstrated a negative percent change from T1 to T2 when compared to Ctx and HC, with no apparent differences between the latter (Fig. 1H; $F_{(2, 44)} = 49.18$, $p < 0.01$; Sidak, Ctx/HC vs. Ext: p 's < 0.01 ; Ctx vs. HC: $p > 0.05$). However, frequency distribution revealed a higher proportion of Ctx rats displaying elevated seeking (Fig. 1I; from T1 to T2: $> -10\%$ change). Rats were further characterized into “more” or “less” seeking from T1 to T2 ($> -10\%$ or $\leq -10\%$ change). Fisher's exact test further revealed significant percentage differences between Ctx and HC (Fig. 1I–J; $p < 0.01$), perhaps indicating the initiation of incubation processes. Together, these results suggest that repeated context exposure during withdrawal may have contributed to worsened withdrawal-associated responses rather than alleviating them by promoting context extinction.

Repeated context exposure alters the NAc-core/shell transcriptome

To identify transcriptional patterns linked to the three WD/Ext conditions, RNA-seq was performed on NAc-core/shell after T2. All conditions were compared to their respective saline group and between NAc-subregions. Surprisingly, the Ctx condition triggered more changes in gene expression (up/downregulation) as compared with the HC or Ext conditions (Fig. 2A). This effect was observed predominantly for the NAc-core. HC and Ext recruited a similar number of DEGs in both NAc-subregions, albeit slightly higher in the NAc-core in the HC group or NAc-shell for the Ext group (Fig. 2A and Supplementary Data 1, DEG lists).

Further examination revealed more upregulated DEGs in NAc-core for Ctx and HC, with more downregulated DEGs in Ext (Fig. 2B). A balanced distribution of up/downregulated DEGs was observed within NAc-shell (Fig. 2B), consistent with NAc-core potentially signaling seeking and NAc-shell perhaps more involved in extinction (inhibitory) processes¹⁵. Cell-type categorization of DEGs identified enrichment for astrocytes and neurons in NAc-core for HC and for microglia in Ext, with less enrichment for Ctx. Within NAc-shell, enrichment for oligodendrocytes, microglia and endothelial cells and neurons was observed in Ctx, HC and Ext, respectively (Fig. 2C; see also Fig. S2A non-specific/annotated DEGs). Biotype analysis showed that the majority of DEGs were protein-coding or predicted genes, with few lncRNAs or miRNAs identified (Fig. 2D; see also Fig. S2B, annotated only). This is unsurprising, given that gene annotation focuses largely on protein-coding genes. To determine overlapping and unique DEGs between WD/Ext modalities in NAc-core/shell, intersectional

Venn diagrams illustrate the far greater number of DEGs in Ctx, with very little overlap seen across abstinence conditions. These findings highlight that distinct clusters of DEGs may drive WD/Ext scenarios in a subregion-dependent manner (Fig. 2E and see also S2C; core vs. shell).

Genome-wide comparisons of transcriptomic patterns across WD/Ext conditions

Given the lack of converging DEGs, we next determined if genome-wide patterns of gene expression—analyzed in a threshold-free manner—were similarly divergent by using rank-rank hypergeometric overlap

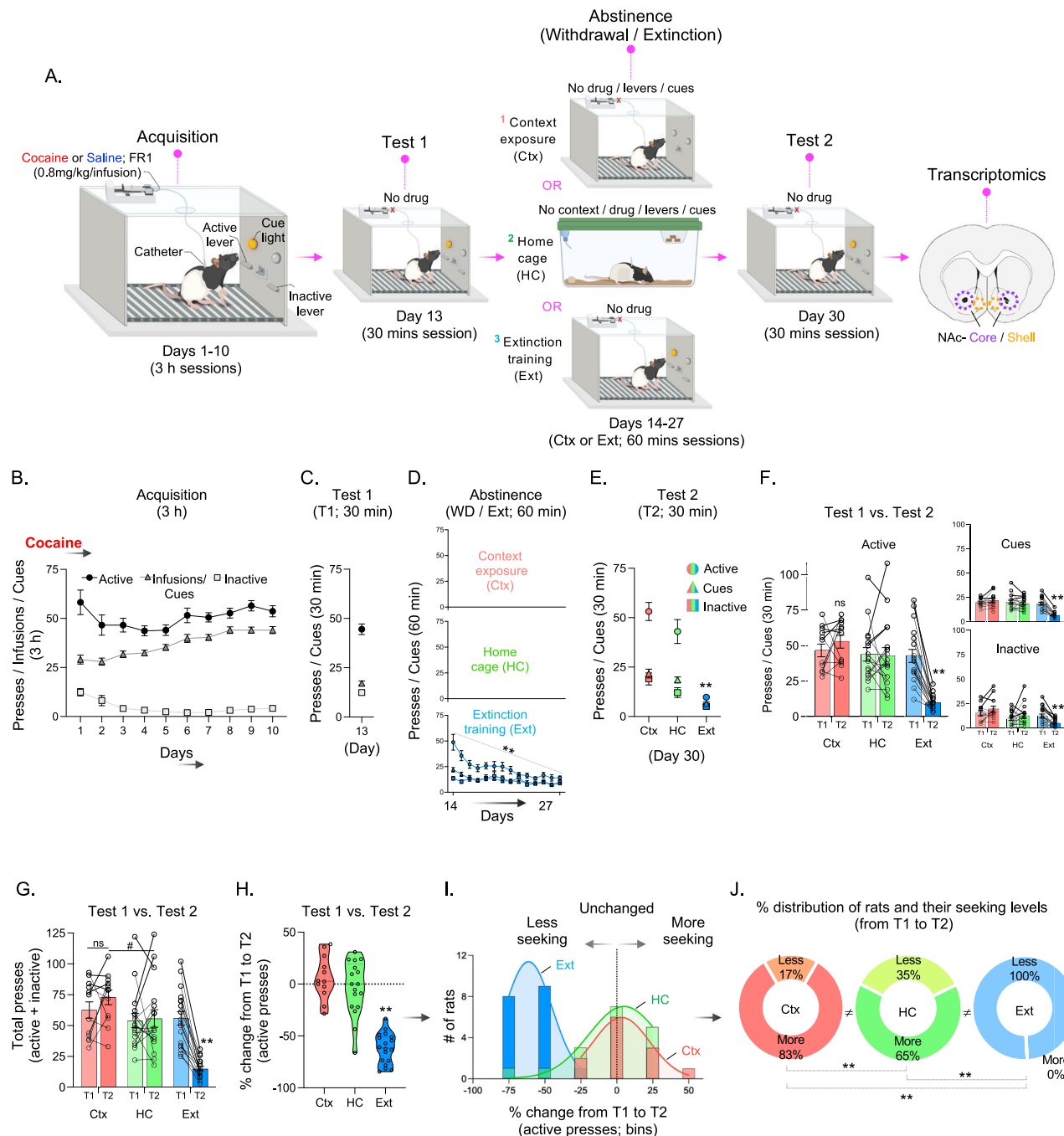


Fig. 1 | Context-exposed withdrawal increases cocaine-associated seeking.

A Schematic depicting experimental design; cocaine withdrawal/extinction (WD/Ext) modalities followed by transcriptomics (RNA-seq) in NAc-subregions.

B, C Acquisition of cocaine SA and Test 1 (T1; drug-free). **D, E** Separation of the experimental groups undergoing WD/Ext in the previous drug context (Ctx), in the home-cage (HC), or under full extinction conditions (Ext), followed by Test 2 (T2; drug-free). Repeated measures and two-way ANOVAs, followed by Sidak post-hoc; $^{**}p < 0.0001$, $^{*}p < 0.0001$, respectively. **F, G** Comparison between Tests 1 and 2 displayed increased (ns), unchanged, and reduced seeking behaviors in the Ctx, HC and Ext groups, respectively. These effects were observed in active and inactive lever pressing (total lever pressing). Repeated measures, followed by Sidak post-

hoc; $^{**}p < 0.0001$, $^{*}p = 0.005$, $^{*}p < 0.0001$ and $^{*}p = 0.10$, $^{*}p < 0.0001$. **H–J** Percent change analysis from Tests 1 to 2 confirms that Ctx-exposed rats trended to display incubation-like behavior, while the HC and Ext groups remained stable or reduced their seeking, respectively (one-way ANOVA, followed by Sidak post-hoc; $^{**}p < 0.0001$). This interpretation was supported by the percentage (%) distribution of rats within the experimental groups (Fisher exact test, $^{**}p = 0.003$, $^{**}p < 0.0001$ (vs. Ext)). Cocaine, Ctx: $n = 12$; HC: $n = 17$; Ext: $n = 18$. All data are shown as mean \pm SEM. $^{**}p \leq 0.01$, $^{*}p \leq 0.05$, $^{*}p \leq 0.10$, ns = non-significant. Created in BioRender. Holt, L. (2025) <https://BioRender.com/l78p336> (HY27SN20NE); Prism 9: GPS-1216108-L###-#####.

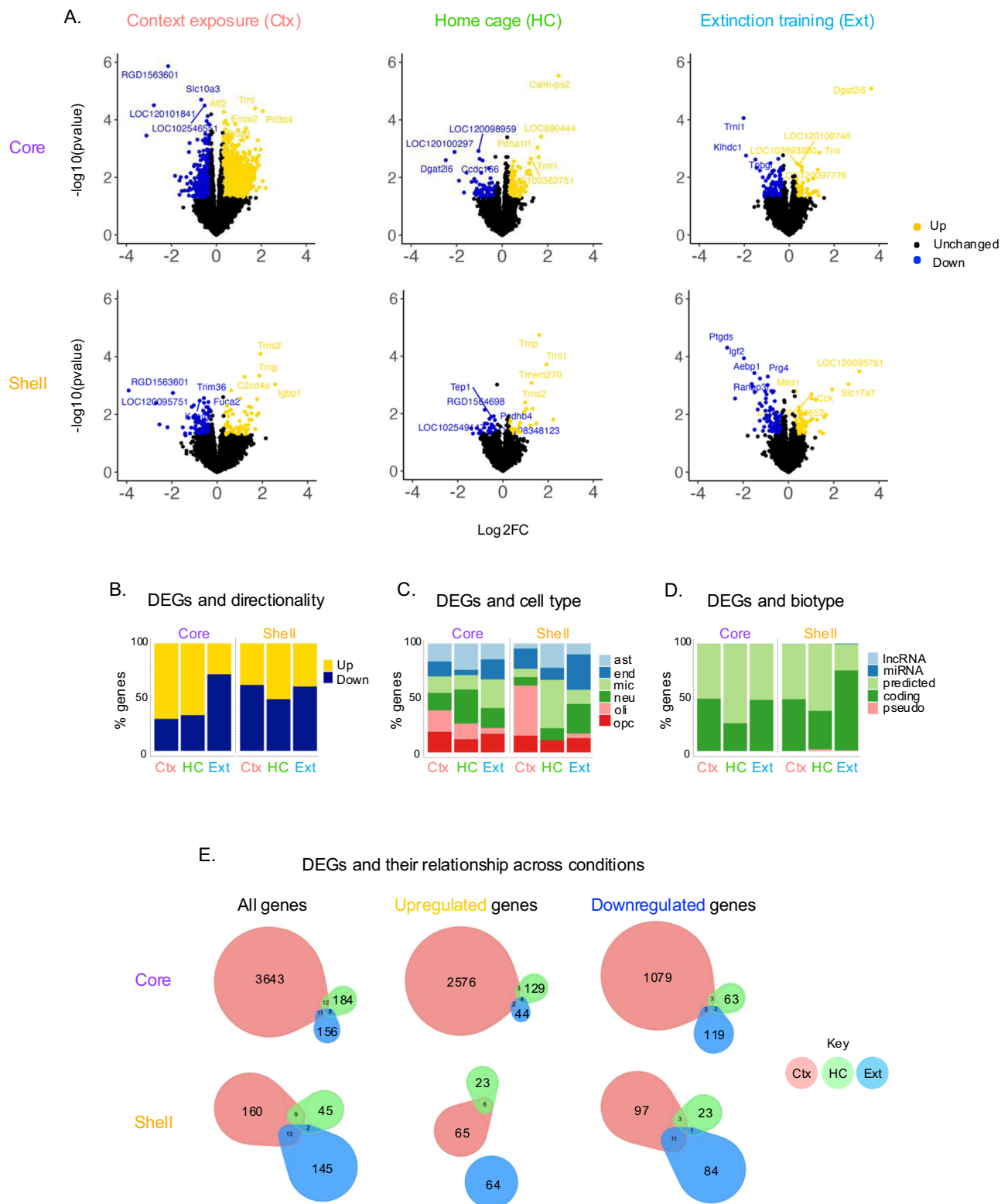


Fig. 2 | Context-exposed withdrawal disproportionately alters the NAC transcriptome. A, B Volcano plots showing differentially expressed genes (DEGs) from WD/Ext conditions for each NAC subregion as compared with their saline counterparts. While the Ctx group showed elevated transcriptional changes in NAC-core (particularly), the Ext group displayed more gene expression changes in NAC-shell. Upregulated and downregulated (nominal $p < 0.05$, $\pm 25\%$ fold-change; 1.25) DEGs are represented in yellow or blue, respectively. Distribution (%) and directionality of DEGs. **C, D** Classification and proportion (enrichment) of DEGs by cell type and

biotype presented across experimental groups for each NAC subregion. Cell types: astrocytes (ast), endothelial cells (end), microglia (mic), neurons (neu), oligodendrocytes (oli), or oligodendrocyte precursor cells (OPC). Biotypes: long non-coding RNA (lncRNA), microRNA (miRNA), predicted encoding genes (predicted), protein-coding genes (coding), non-protein-coding genes (pseudogene). **E** Venn diagrams depicting the proportion of DEGs and their relationship (shared/overlapping) across WD/Ext conditions and NAC-subregions.

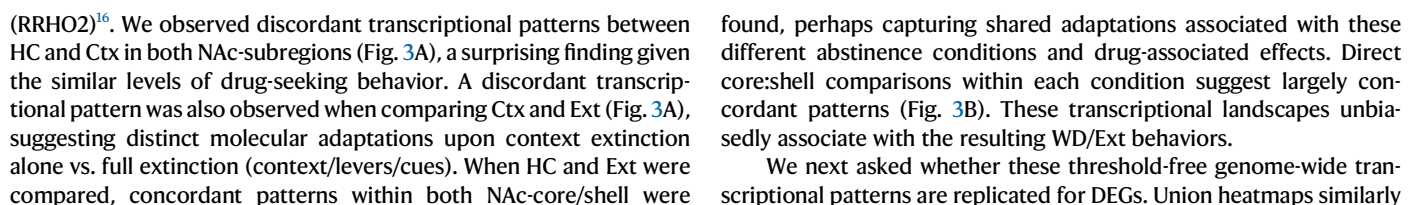


Fig. 3 | Gene expression patterns across WD/Ext conditions and NAc-subregions. **A** Global threshold-free comparisons of gene expression by Rank-Rank Hypergeometric Overlap (RRHO2) plots showing the degree of transcriptional concordance/discordance across conditions and regions. A strong discordance was observed when the Ctx group was compared with either the HC or Ext group, while HC and Ext displayed transcriptional concordance. **B** Both of these patterns were seen in NAc-core/shell. Concordance is indicated by the distribution of genes in the bottom left and top right quadrants denoting co-upregulation (yellow arrows in key) and co-downregulation (magenta arrows in key), respectively. Discordance is indicated by the distribution of genes in the top left and bottom right quadrants indicating oppositely regulated genes (up-down; yellow/magenta arrows and

down-up; magenta/yellow arrows, respectively). The overlapping intensity is color-coded, where genes are sorted from most to least significant from middle/center to corner in each quadrant. **C** Union heatmaps generally confirm these RRHO2 patterns by displaying the distribution of all DEGs (upregulated: yellow or down-regulated: blue), where the Ctx group displays little overlap with the other two groups. **D** Alluvial plots highlighting clusters of DEGs with expression patterns across conditions and NAc-subregions. Plots are stratified by behavioral condition (x-axis) to display the number of DEGs assigned to each pattern/cluster/alluvium (color-coded). Upregulation (upward arrow), downregulation (downward arrow), non-significant (ns) and variable indicate a combination of upward and downward arrows or ns (no relationship/overlap) for each condition.

depicted divergent patterns between Ctx and the other conditions (Fig. 3C). Also consistent with the RRHO2 analysis, HC and Ext shared similar fold-change patterns of gene expression. Alluvial plots depicted the flow of DEGs in seven different dynamic clusters that captured concordance in at least two conditions (Fig. 3D, non-gray colors), or variable patterns across conditions (gray curves). For instance, the yellow cluster (NAc-core) demonstrates concordant upregulation in HC and Ext, consistent with RRHO2 results. The purple cluster demonstrates concordant downregulation between Ctx and Ext, as in the heatmaps (Fig. 3C; NAc-shell).

Predicted biological functions, upstream regulators and transcription factors in NAc-subregions across WD/Ext conditions

We bioinformatically assessed key regulatory mechanisms associated with gene expression. We first used Gene Ontology (GO) analysis to link DEGs with known biological functions (Fig. 4A and Supplementary Data 2). Top GO terms for NAc-core implicated growth factors and extracellular matrix (Ctx) and RNA biosynthesis (HC and Ext). In contrast, NAc-shell associated with DNA replication and receptor signaling/transactivation (Ctx and HC) and extracellular matrix (Ext). Interestingly, Venn diagrams revealed minimal overlapping of biological functions across conditions and NAc-subregions (Figs. 4B and S3A), again supporting the involvement of distinct molecular mechanisms across WD/Ext conditions. Examination of the regulation status of genes within each GO term particularly displayed a balanced (core) or downregulation (shell) status for Ctx, a strong upregulation in HC and a broad downregulation in Ext (Fig. S3B). GO analysis on clustered DEGs further revealed molecular mechanisms underlying the behavioral adaptations (Fig. S4A, B).

To identify regulatory factors, we used Upstream Regulator Analysis (IPA). Union heatmaps display regulators found in at least two of the three conditions (Fig. 4C and Supplementary Data 3). Despite concordant global transcriptional patterns between Ext and HC (see RRHO2, Fig. 3A), we observed more overlap between Ctx and Ext and few predicted regulators in HC (Fig. 4C). Additionally, within the core, half (34/65) demonstrated opposing activation status. Given the lack of overlapping DEGs, it is not surprising that different regulators are implicated in Ctx and Ext (Fig. 4C). For instance, differential status between Ctx and Ext conditions was observed (Fig. 4C) in JUNB (NAc-core), FOS (NAc-shell), and ESRI and 2 (estrogen receptors; core/shell), whereas RARA (retinoic acid receptor- α) and RGS4 (regulator of G protein signaling-4) were among the identified factors in HC (NAc-core). Interestingly, downregulation of estrogen receptors (ESRI/2), also previously linked to responsiveness to cocaine¹⁷, was captured in Ext (Fig. 4C).

We next turned to motif enrichment and discovery analyses (MEME Suite; SEA) to identify upstream transcription factors. The top 30 transcription factor motifs deduced demonstrated little overlap between behavioral conditions (Fig. 5A), similar to IPA analysis. The identified factors were particularly driven by Ctx (NAc-core), potentially suggesting subregion-specific transcriptional regulation. We identified enriched putative motifs for ZNF263 (Ctx) and RRBE1 (HC), proteins associated with drug exposure^{18,19} (Fig. 5B, left/middle panels). In Ext, enrichment of transcription factors (motifs) was

observed in the NAc-shell (Fig. 5A), consistent with extinction processes. Among the top factors, ZNF263 and SP2 were observed, both related previously to drugs^{18,20} (Fig. 5B, right panels).

Divergent gene co-expression networks across NAc-subregions and WD/Ext conditions

We next used MEGENA to determine co-regulated genes and hierarchical gene modules (sunburst plots; Fig. 6A). This revealed minimal overlap of modules when Ctx is compared to either HC or Ext (Fig. 6A, NAc-core, left/middle panels). By contrast, several gene modules displayed overlap between HC and Ext (Fig. 6A, NAc-core, right panel), supporting the uniqueness of Ctx. Similar, although weaker in magnitude, results were observed under saline conditions (Fig. S5A). In contrast, NAc-shell displayed overlapping modules between Ctx and the other groups (Fig. 6A, NAc-shell, lower panels), suggesting subregion-dependent patterns of regulation. NAc-shell showed little overlap under saline groups, suggesting cocaine-specific effects. A small number of modules exhibited overlap for global core:shell comparisons (Fig. S6A, B).

ARACNE identified gene regulatory interactions and targets mediated by transcription factor binding and reconstruction of associated networks (Fig. 6B, C). In NAc-core (Figs. 6B and S7A), small nucleolar RNAs (e.g., *LOC* genes; module C1_5) were central to Ctx vs. HC (Fig. 6B, left panel), whereas myelin-associated glycoprotein (*Mag*; module C1_3) and other hub genes including *Scn11A* (sodium channel subunit), *Esrrb* (estrogen receptor) and *Plcg2* (phospholipase C γ) (module C2_122) were central to HC vs. Ext (Fig. 6B, middle/left panels, see also Fig. S7A). As for NAc-shell (Figs. 6C and S7B), nuclear ribonucleoprotein (*Hnrnpu*; module C1_37) was central to Ctx and HC (Fig. 6C, left panel), whereas calcium/calmodulin-dependent kinase (*Camkv*, module C1_2), heat-shock proteins (*Hsp90ab1*; module C1_6) and ATP synthesis (*Apt5fla/b*; module C1_7) were among the overlapping hub genes for Ctx and Ext (Fig. 6C, middle panel and Fig. S7B, left panel). HC and Ext revealed genes involved in cell membrane dynamics (membrane-associated ring finger; *March10*; module C1_126), cation-chloride transport (*Slc12a8*; module C1_253) and other unspecified genes (e.g., *LOC* genes; module C1_98) (Figs. 6C and Fig. S7B, right panels). Several of these hub genes (e.g., *Camkv*, *Hnrnpu* and *Mag*) have been associated with cocaine exposure^{21–27}.

Comparison of transcriptional regulation in rat NAc across WD/Ext conditions to transcriptional abnormalities in NAc of human CUD

We recently demonstrated transcriptomic convergence in NAc between cocaine SA in mouse and CUD in humans⁹, but such convergence has never been examined across WD/Ext conditions and NAc-subregions. We, therefore, proceeded to compare global transcriptomic expression patterns, DEG distribution and GO analysis of rats to humans who died after cocaine overdose (Fig. 7A). RRHO2s revealed genome-wide concordance between rat Ctx and CUD in both NAc-core and NAc-shell, whereas HC and Ext showed discordance to CUD (Fig. 7B), patterns that were also observed in DEGs (Fig. 7C, core/shell). A notable overlap in downregulated genes was apparent for all

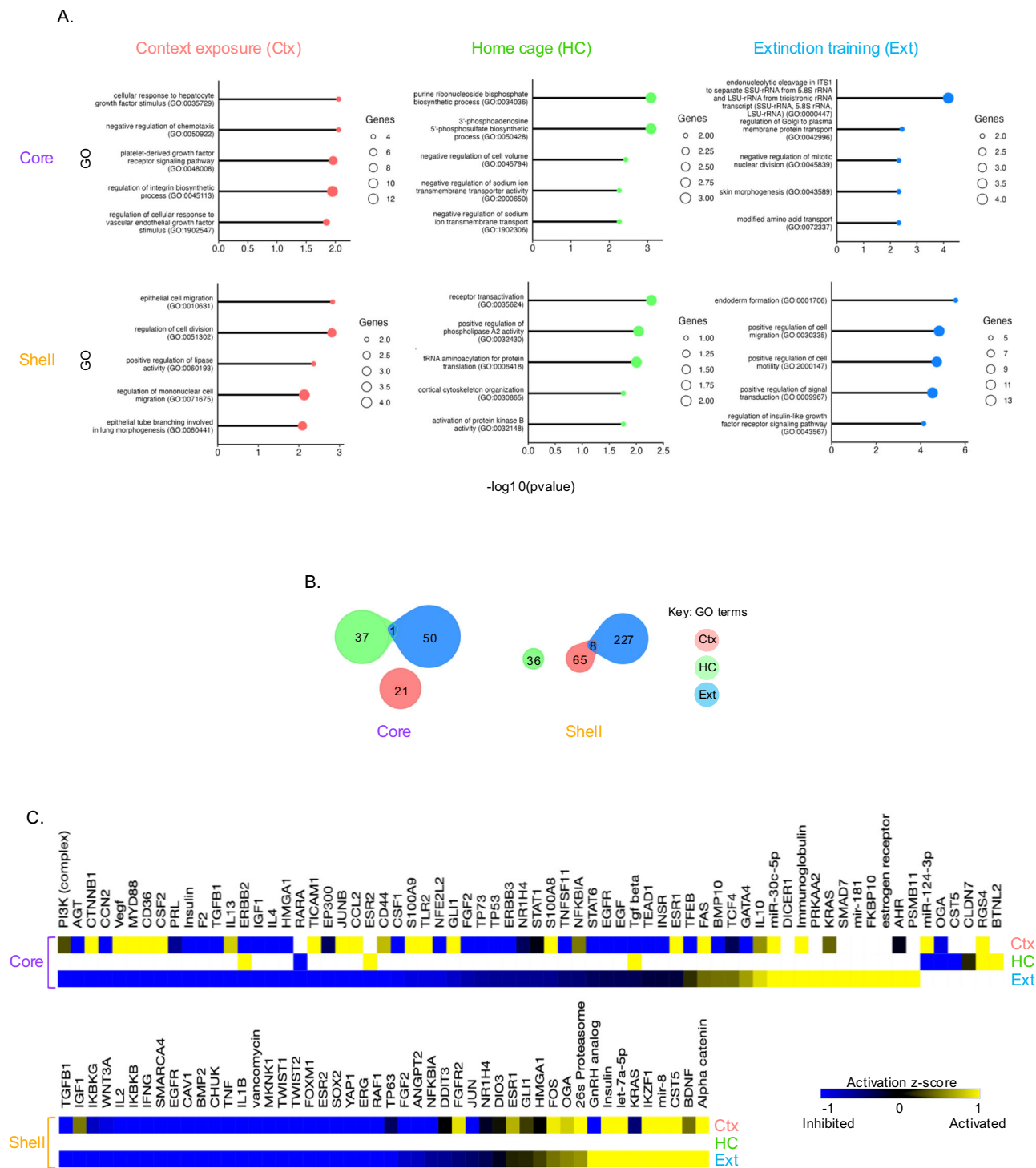


Fig. 4 | Predicted biological functions and upstream regulators across WD/Ext conditions and NAc-subregions. A Top gene ontology (GO) terms in NAc-core featured enrichment of DEGs associated with growth factors, integrins regulation (Ctx) and RNA biosynthesis (HC and Ext), while NAc-shell was implicated in cell division, DNA replication, receptor signaling/transactivation (Ctx and HC) and extracellular matrix dynamics (Ext). Dot size is reflective of the number of genes per gene ontology term. **B** Venn diagrams highlighting different GO term distribution

across conditions with the Ext group involving a higher number of biological functions. **C** Upstream regulator analysis linked numerous putative regulators to the seeded DEGs with activation or suppressive properties across the WD/Ext conditions in NAc-core or shell. Activation z scores: Activated (yellow) = over-representation of targets activated by the regulator; Suppressed (blue) = over-representation of targets repressed by the regulator; black/gray = not a predicted upstream regulator.

conditions, which was not detected by RRHO2 (Fig. 7C, core/shell). Venn diagrams revealed a subset of shared DEGs; GO analysis revealed several top overlapping GO terms represented (e.g., phospholipid processes, GTPase activity, cytokine signaling, histone acetylation and calcium signaling) (Fig. 7D–F, Supplementary Data 4). Several of these

genes (e.g., *SAMD3*, *HTR7*, *PPP1R17*)^{28–32} and upstream regulators (e.g., STAT3, AR, mir-124) have been associated with cocaine exposure^{33–36}. Together, these results suggest that the Ctx condition more similarly captures NAc transcriptional patterns observed in human CUD compared to HC and Ext paradigms.

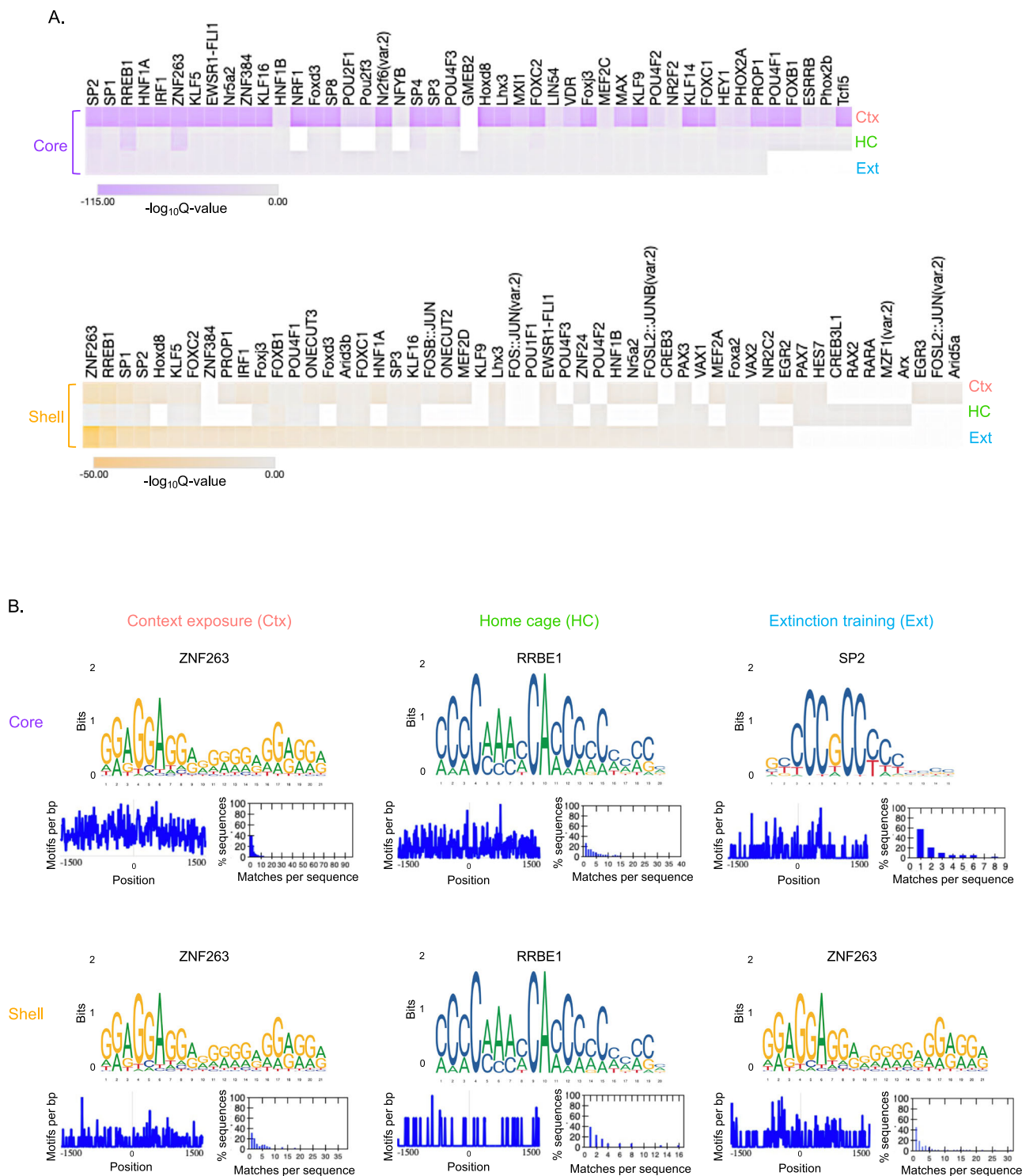


Fig. 5 | Motif enrichment analysis and identification of DNA binding factors across WD/Ext conditions and NAC-subregions. A Top transcription factors deduced (seeded) across WD/Ext conditions and NAC-subregions obtained by Simple Enrichment Analysis (SEA) of DEGs. The identified motifs were overwhelmingly linked to putative factors in the Ctx group within NAC-core, while elevated incidences in NAC-shell were observed for the Ext group. The Q-value

represents the minimum false discovery rate (FDR) required to consider a motif significant. **B** Representation of selected (top) individual motifs (logos, positions and incidence/matches) and their binding factors. Positional distribution of the best match to the motif in the primary sequences. The dotted line indicated the position of the sequences aligned to the left/right ends or centers. The histograms show the number of motif matches in the primary sequence with at least one match.

Discussion

In this study, we used cocaine SA in rats to unveil behavioral and transcriptional patterns of forced abstinence scenarios involving distinct withdrawal or extinction modalities. We identified numerous transcriptome-wide changes in the core and

shell subregions of NAC that associate with the addictive continuum in rats that experienced cocaine withdrawal in their home-cage or in the previous drug context, or experienced full extinction conditions. Of particular interest was the observation of enhanced drug seeking in rats undergoing context withdrawal,

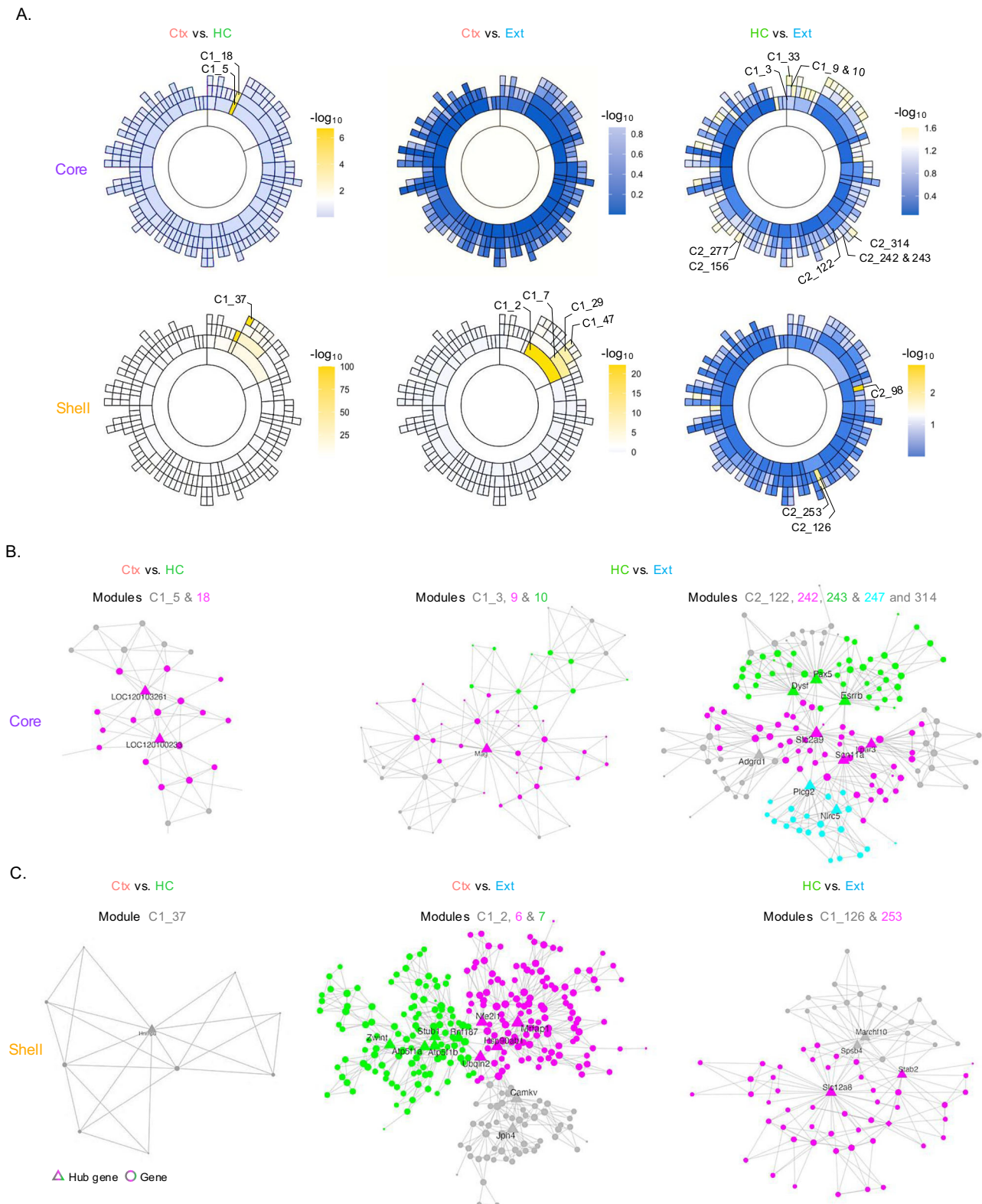
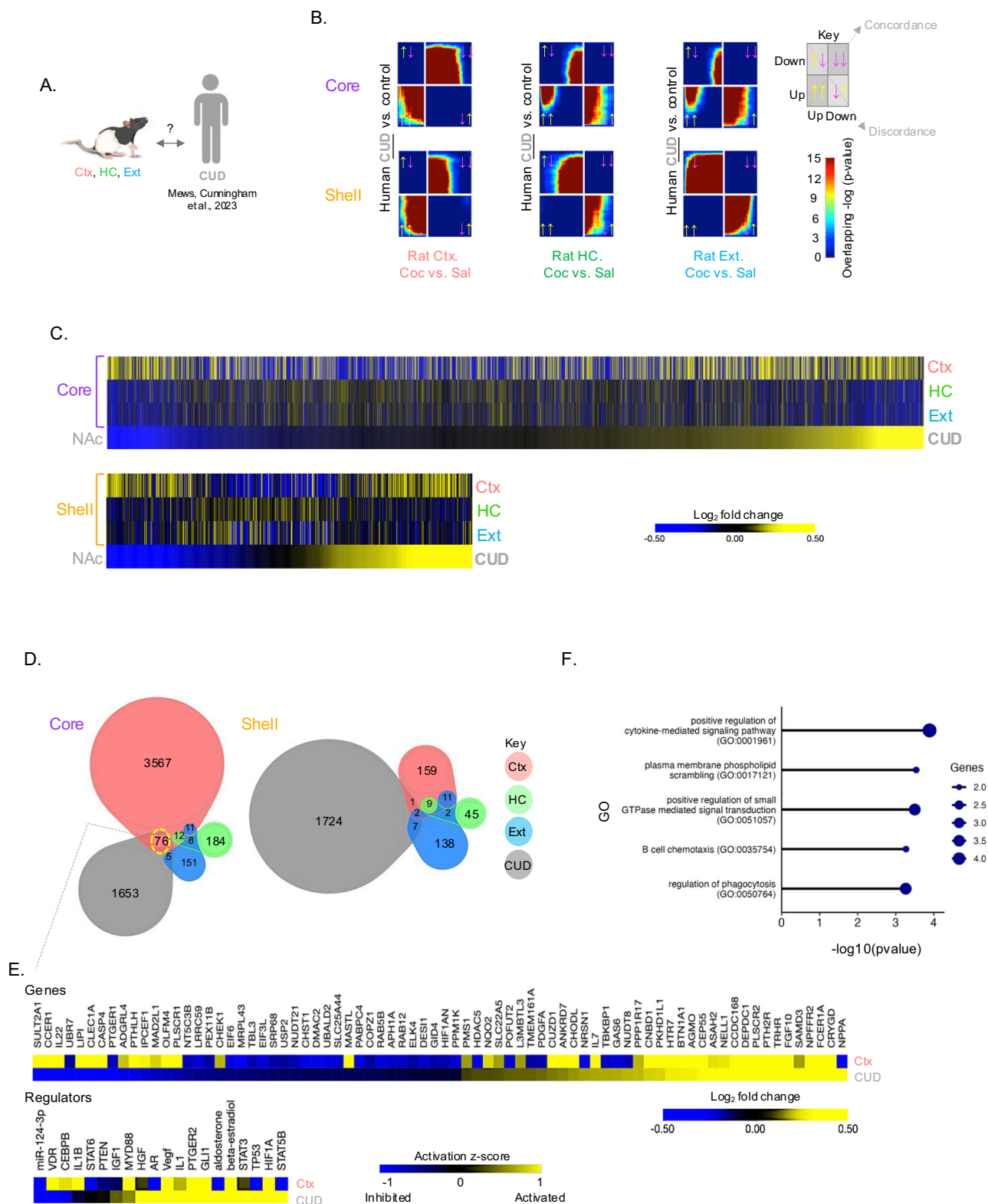


Fig. 6 | Co-expression network analysis across WD/Ext conditions and NAc-subregions. A Sunburst plots, depicting gene (DEGs) co-expression networks by MEGENA in cocaine-exposed groups, show little overlap (white/blue modules) when the Ctx group is compared with the HC or Ext groups (core/shell; left and middle panels). Still, the presence of overlapping gene modules was observed (yellow modules). Comparison between HC and Ext conditions revealed several shared gene modules (yellow), particularly in NAc-core (top-right panel). Inner and

outer rings of the sunburst plots are referred to as parent and child modules, respectively. **B, C** ARACNE plots showing gene network and connectivity within some of the overlapping modules across WD/Ext conditions and NAc-subregions. The colors of symbols represent module assignment. These networks also highlight hub/driver and other highly connected genes; symbols reflect hub drivers versus connected genes (triangle = hub gene; circle = gene).



whose NAc transcriptional profiles converged with those of humans with CUD.

Forced abstinence modalities

Withdrawal and extinction phases have been studied in animals for decades^{5,37,38}. These strategies have centered largely on applying forced abstinence either in home cages or under full extinction conditions. Full extinction training involves dissociating the prior drug

context, levers and cue lights from drug access. However, a partial form of extinction is also possible, wherein animals are exposed repeatedly to the previous drug context, but with the omission of drug-associated triggers (e.g., levers and cue lights). Here, we directly compared all three of these preclinical models at the behavioral and transcriptional levels.

Contextual extinction paradigms have been found to reduce associated responses, for example, for fear conditioning or cocaine-

Fig. 7 | Convergent transcriptional patterns in NAc between Ctx withdrawal in rats and human CUD. **A** Schematic posing the comparison between WD/Ext modalities in rats and human CUD. **B** RRHO2 plots reveal a robust and global transcriptional concordance between Ctx rats and CUD (left panels core/shell) and predominant discordant patterns when CUD is compared against HC or Ext groups (middle and right panels core/shell). Concordance/ Discordance; same or opposite direction of yellow /magenta arrows. **C** Union heatmaps showing a similar distribution of DEGs between CUD and Ctx groups, which is consistent with the RRHO2 results. Upregulation: yellow or downregulation: blue (nominal $p < 0.05$, $\pm 25\%$ fold-change; 1.25). **D** Venn diagrams showing the proportion of DEGs and their relationship (overlap) between CUD and WD/Ext conditions in NAc-subregions. Note that the CUD data were obtained from whole NAc encompassing both

subregions (Mews and Cunningham et al.⁹). **E** Union heatmaps (upper panel) highlighting the shared genes and their expression direction (up = yellow, blue = down) between CUD and Ctx datasets, as well as the consequent upstream regulators for NAc-core. Activation z scores: Activated (yellow) = overrepresentation of targets activated by the regulator; Suppressed (blue) = overrepresentation of targets repressed by the regulator; black/gray = not a predicted upstream regulator. **F** Overlapping top gene ontology (GO) terms between CUD (whole NAc) and across WD/Ext conditions in NAc subregions with a notable enrichment of DEGs associated with cytokine, GTPase and plasma membrane signaling. Dot size is reflective of the number of genes per gene ontology term. Created in BioRender. Holt, L. (2025) <https://BioRender.com/q81g274> (MS27SN28G4).

conditioned place preference^{39–41}. We demonstrate, in contrast, the opposite effect with cocaine SA. Ctx increased drug-seeking behavior to the level at or greater (to some extent) than home-cage abstinence. It is possible that repeated context exposure increased drug-seeking behavior by initiating or potentiating the incubation of craving as observed during cue/context-induced relapse⁴². Another possibility is that drug contexts act as “occasion setters”³ and are not valued equally compared to drug-associated instruments or cues linked to the drug itself. This is also different from conditioned place preference scenarios, where context is the only drug association. Thus, repeated omission of instruments/cues in the original context could lead to increasing the expectation of obtaining the drug.

Full extinction training, on the other hand, simultaneously extinguishes all drug-paired stimuli⁴³. Still, a key challenge is knowing whether the animals refrain from drug seeking because they learned the lack of drug availability or because they reduced craving/motivation per se. Our observed increase in drug seeking after context-only exposure in rats is consistent with the limited clinical success of extinction training⁴⁴. Subjects commonly develop compulsive drug taking in a given context, learn extinction in a different (clinical) setting and often relapse upon returning to the original context/cues. To our knowledge, the present study directly compares these three WD/Ext modalities in male rats. Future research is needed to determine whether similar patterns hold for females and under other context-associated paradigms (e.g., renewal/ABA).

Transcriptional programs in NAc under forced abstinence modalities

We show that the three WD/Ext procedures associate with highly distinct transcriptomic patterns in the NAc-core and NAc-shell. Notably, context exposure (Ctx) induced the strongest transcriptional burden with a particular upregulation of genes (e.g., NAc-core). This was accompanied by biological functions involved in sterol (lipid) metabolism and membrane (integrin, receptors, lipids) regulation, processes impacted in drug addiction^{45–49}, as well as upregulation of key upstream regulators, such as JUNB, estrogen receptors (core) and FOS (shell), that are also implicated in addiction^{50,51}. For instance, we uniquely observed upstream activation of immediate early gene products JUNB (Fig. 4C, upper/NAc-core panel) and FOS (Fig. 4C, lower/NAc-shell panel) in Ctx conditions with inhibition in Ext and no change in HC. Such patterns may reflect unique changes in neuronal activity that support elevated seeking behavior in Ctx withdrawal, as both NAc-core and -shell have been implicated in seeking behaviors and drug-associated contexts^{52,53}. In parallel, activation of BDNF under Ext and no change in Ctx could signal extinction learning⁴⁷ (Fig. 4C, lower/NAc-shell panel).

In parallel, activation of BDNF under Ext and no change in Ctx could signal extinction learning⁵⁴ (Fig. 4C, lower/NAc-shell panel). RARA (retinoic acid receptor- α) and RGS4 (regulator of G protein signaling-4) were identified in HC and previously associated with cocaine exposure^{55,56} (Fig. 4C, upper/NAc-core panel). Interestingly, estrogen receptors (ESR1 and 2) were predicted to be activated in Ctx and HC groups (NAc-core) and inhibited following Ext (NAc-core)

(Fig. 4C, core/shell). Increased levels of 17 β -estradiol are postulated to facilitate increased sensitivity of females to cocaine compared to males, and estradiol treatment of males increases acquisition of cocaine self-administration in male rats^{17,57}.

Motif analysis from Ctx revealed singular enrichment for transcription factors in core/shell subregions, which largely differed between Ext and HC animals. This discordance suggests that extinction training may counteract key features of withdrawal and relapse⁵⁴. However, the unexpected transcriptional discordance between context and home-cage withdrawal, when both conditions associate with drug-seeking behavior, suggests that different biological pathways contribute to relapse and that the withdrawal context matters^{6,43}.

A surprising finding was the observation of some concordant gene expression patterns between home-cage withdrawal and extinction training. Such transcriptional convergence between these two conditions could represent shared withdrawal-associated, or craving-associated, changes in NAc despite extinction training. Nonetheless, a closer look at the distribution of DEGs, regulators and biological functions highlights clear transcriptomic differences for NAc-core and -shell. These findings raise the possibility that different gene expression patterns associated with specific WD/Ext experiences may still lead to similar behavioral outputs. Social defeat stress reveals a comparable scenario, wherein mice that exhibit resilience to stress demonstrate similar behavioral outputs to control (non-stressed) mice despite very different transcriptomes⁵⁸. Although this could be region dependent, this is a very interesting finding, since no other study has directly shown these comparisons in WD/Ext conditions. In addition, the time that passed after the WD/Ext tests and the tissue collection as well as the differential gene expression analysis (e.g., uncorrected vs corrected p -values) may have impacted these genome-wide expression patterns. Some of these differences could reflect contextual withdrawal differences, but importantly our corresponding saline controls accounted for the context and instruments/cues independent of the drug.

Gene co-expression networks in NAc-subregions across WD/Ext conditions

Transcriptomic differences between NAc-core and NAc-shell during abstinence have not been previously characterized. Here, threshold-free RRHO2 revealed concordant gene expression patterns between these two NAc subregions, whereas DEG-based analyses revealed pointed transcriptional differences across the behavioral scenarios. For instance, Venn diagrams displayed little DEG overlap between core and shell (Fig. S2C), an effect that was also observed by gene ontology (Fig. S3A). Such discrepancies between RRHO2 and DEG analyses suggest broad convergence in transcriptional regulation in NAc-core and NAc-shell, but with differences in the magnitude and consistency in individual gene changes in the two regions such that many changes reach statistical significance in only one subregion. These differences in statistical significance would appear to be biologically relevant given different roles demonstrated for NAc-core and NAc-shell^{15,59,60}. For example, the upstream regulator analysis indicated BDNF as an

activated regulator following extinction in NAc-shell, which agrees with other studies and emphasizes BDNF's involvement in extinction learning^{54,61}. Although this evidence varies by behavioral approaches and testing time points, brain regions, drug studied and cellular/molecular techniques, the findings converge on BDNF's role in extinction processes (for review see also refs. 62–64).

We additionally identified potential upstream regulators associated with differential gene expression. GLII (glioma-associated homologue-1, activated in Ctx from NAc-core; Supplementary Data 3), a zinc-finger transcription factor, is in-part regulated by estrogen^{65,66} and is a predicted upstream regulator of FOS expression, both implicated in our dataset. The direction of activation for these regulators occurs in the same direction, and several target DEGs were found to be overlapping (AKT1, EGFR, FOS, HES1, IGF1 to name a few). GLII is known to activate mTOR pathway⁶⁷, shown to be important for behavioral sensitization to cocaine within the NAc⁶⁸. TWIST1 and 2 were inhibited upstream regulators in both subregions across Ctx and Ext conditions, and their role in cocaine drug-seeking is currently unknown. Downregulation of Twist1 decreases neurotoxicity associated with huntingtin protein overexpression in cultured primary neurons⁶⁹; perhaps inhibition of these zinc-finger binding domain proteins is a compensatory mechanism to mitigate cocaine's neurotoxic effects. Motif analyses also display enrichment of several zinc finger proteins, BDNF signaling (e.g., CREB being downstream of BDNF), and transcription factors like FOX and FOS/JUN, all relevant for drug plasticity^{70,71}. This analysis additionally identified transcription factor motifs such as ZNF263, enriched in Ctx from NAc-core and Ext from NAc-shell. ZNF263 is linked to extracellular matrix protein biosynthesis, in line with our GO results (Fig. 4A). Enrichment of RRBE1 implicates MAP kinase signaling, which has been previously involved in glutamatergic plasticity in the NAc following cocaine withdrawal⁷².

Network analysis revealed minimal overlap between gene co-expression modules for NAc-core and NAc-shell, opening a way to search for unique hub genes. To this end, we identified several hub genes associated with small nucleolar RNA (some *LOC* genes) and ribonucleoproteins (*Hnrnpu*), key in RNA processing (e.g., methylation/uridylation), that stand out when Ctx and HC are compared, highlighting potentially common withdrawal features compared to extinction. Gene co-expression between Ctx and Ext reveals cell signaling (*Camkv*) and metabolism processes (*Atp5f*), perhaps critical to instrumental or contextual WD/Ext learning. Overlapping results between HC and Ext identified several genes involved in ion transporters and channels (*Slc12a8/9*, *Scn11a*), estrogen action (*Esrrb*) and myelin (*Mag*), potentially signaling spontaneous extinction- or withdrawal-associated processes.

Transcriptional convergence in NAc between rat WD/Ext and human CUD

Capitalizing on recent human studies, we integrated the present rat transcriptional dataset with the NAc transcriptomes from individuals with CUD who died from cocaine overdose⁹. This integration identified gene signatures that are translationally significant for understanding CUD. Notably, Ctx animals showed convergence in their global transcriptome with that of CUD, characterized by shared DEGs and upstream regulators. Examples include gene targets such as *Htr7*, *Fgf10*, *Samd3* and *Pabpc4* and upstream regulators GLII; and previously identified targets such as NPFFR2, STAT3³³, estradiol⁷³ and mir-124-3p⁷⁴. Conversely, HC-withdrawal and extinction diverged from the CUD transcriptome, a discrepancy that may mirror the specific addiction stage in which CUD subjects died.

The last instance of drug exposure differed between Ctx (after WD) and CUD (after overdose) groups, and thus our results might reflect a molecular landscape that supports drug craving to drive drug-seeking behavior during withdrawal rather than the acute effects of cocaine. For instance, we observed a smaller proportion of HC animals

classified as increased seeking after withdrawal compared to Ctx. HC animals demonstrated largely discordant, with some concordant gene expression with human CUD. Mews and Cunningham et al.⁹ also reported more transcriptional convergence between CUD and 24-h cocaine withdrawal compared to acute cocaine exposure in mice. Comparisons of rodent models to human CUD patients at different stages of the addiction cycle (e.g., with and without withdrawal or relapse) is an important priority for future work.

Although home-cage abstinence is the gold standard approach to studying withdrawal in rodents, the fact that the Ctx group converges the most with the human CUD data suggests especially strong validity of this form of abstinence in modeling key aspects of CUD. Moreover, the fact that extinction associates with unique expression patterns supports the strategy of using extinction-based approaches as a preferred non-invasive treatment for SUDs⁷⁵. Future research should pinpoint cell-specific⁷⁶ regulatory mechanisms (e.g., epigenetics)⁷⁷ linked to these behavioral states, including relapse or context renewal, and extend it to additional brain reward regions.

As molecular biological and bioinformatic analyses progress, the use of these preclinical approaches is fundamental to modeling some of the most devastating features of SUDs. The transcriptome-wide mapping of gene expression changes in the rat NAc-core and NAc-shell induced by three very different abstinence conditions provides biological insight into CUD. Our findings also highlight how transcriptomic profiling might be used to formulate and perfect behavioral strategies (e.g., extinction-based training) to counteract specific aspects of withdrawal and relapse. Future studies focused on the functional role of key hub genes will be important to establish the role played by these candidate genes in driving specific behavioral features of WD/Ext behaviors.

Methods

See the Supplementary Section for full methodological descriptions.

Animals

Male Long-Evans rats (8–12 weeks) were maintained on a 12-h reverse light-dark cycle with food and water ad libitum. Experiments were executed during the dark phase (13:00–18:30) under red light illumination. Rats were restricted to 18 g/day of chow. All procedures were approved by the Institutional Animal Care and Use Committee and the Association for Assessment and Accreditation of Laboratory Animal Care.

Jugular vein catheterization (JVC)

Under isoflurane anesthetization (5% induction, 2–3% maintenance), catheters were implanted in the right jugular vein as described previously⁷⁸ with daily 0.1 ml heparinized saline (30 U) containing ampicillin (5 mg/ml) flushing during recovery days 4–7. The analgesic (carprofen, 5 mg/kg) was administered subcutaneously. Catheters were tested for patency using methohexital (Brevital; 5 mg/kg).

Drug

Cocaine HCl (NIDA) was dissolved in saline during SA (acquisition).

Operant boxes

Cocaine (or saline) was SA from a syringe pump in operant boxes controlled by an interface system (Med Associates).

SA phases (acquisition, Test 1, withdrawal/extinction and Test 2)

Acquisition: Rats were trained to SA cocaine (0.8 mg/kg/infusion) on an FR1 ratio during 3-h sessions over 10 days⁷⁸. Infusions/rewards were signaled by a cue light above the active lever followed by a 20-s timeout period in which the light remained illuminated and levers extended. Inactive lever presses were recorded but had no consequences. **Test 1 (T1):** Two days after acquisition, rats were placed in the operant boxes under full extinction conditions (no drug) for 30-min.

The next day, rats were separated into three WD/Ext groups for 14 days. 1) *Context exposure (Ctx)*: daily exposure to the previous drug context (1-h sessions) but without levers, cues or drug. 2) *Home-cage (HC)*: Rats were kept in their home-cages and handled daily in the behavioral rooms. 3) *Extinction training (Ext)*: daily 1-h sessions with access to the context, levers, and cue light but without drug infusions.

Test 2 (T2): Two days after the WD/Ext sessions, rats were placed in the operant boxes for 30-min and lever presses were recorded.

Tissue collection

Thirty minutes after Test 2, rats underwent live decapitation where the brains were extracted, sliced and bilateral punches of NAc-core and -shell (separately) were collected⁷⁹, flash-frozen on dry ice and stored at -80°C . The total time (including the test = 60 min) is when immediate early gene expression peaks and coincides with peak transcriptional expression associated with drug-seeking behaviors as previously observed^{50,76,80–83}.

RNA isolation and library preparation

Total RNA was isolated using Direct-zol RNA kit (Zymo Research, CA). RNA quality and concentration were evaluated using Bioanalyzer (2100; Agilent Technologies, CA) and Nanodrop (Thermo-fisher, MA). SMARTer Stranded Total RNA-seq kit v3-Pico Input Mammalian (Takara Bio, CA) was used for library preparation. All libraries were tested for quality control (Bioanalyzer)^{84,85}.

Sequencing and differential expression gene analysis

Sequencing was performed by Genewiz/Azenta (MA) on Illumina NovaSeq instrument with a 2×150 bp paired-end read configuration and 30 M reads per sample. Alignment and trimming were performed (rn6-GCF_000001895.5) using the NGS-Data-Charmer pipeline (<https://github.com/shenlab-sinai/NGS-Data-Charmer>). We used GENCODE vM25 annotation for counts of mapped reads. Differential expression analysis was performed (removing low-count genes; <6), yielding a total of 29,888 genes using the DESeq2 R-package (4.0.2). Significance for differentially-expressed genes (DEGs) was set at a fold-change (LogFC) of $\pm 25\%$ and nominal $p < 0.05$ (Supplementary Data 1; reporting uncorrected/nominal and corrected/adjusted p -values)^{9,50,86–88}. This is also available in the Gene Expression Omnibus (GEO) database repository (accession number: GSE264129).

Biotype and cell type

The Ensembl *biomaRt* R-package was used to categorize DEG biotypes. For cell-type enrichment, DEG lists were integrated with a single-cell RNA-seq database⁸⁹, which classifies genes enriched in astrocytes, endothelial cells, microglia, neurons, oligodendrocytes, or oligodendrocyte precursor cells. Specifically, DEG lists were classified based on the “top cell-type-specific” category from McKenzie et al., whereby expression of the gene is several-fold higher in one cell type vs. all others⁸⁹.

Volcano plots and union heatmaps

Volcano plots were generated in R (v4.0.2) using ggplot (v3.4.2). Venn diagrams were generated using R (v4.0.2) using Venn⁹⁰. Union heatmaps of DEGs merged by Log₂FC of each condition were generated using Morpheus (<https://software.broadinstitute.org/morpheus>).

Rank-rank hypergeometric overlap (RRHO2)

Stratified, two-sided RRHO2 plots were generated using the RRHO2 R-package (github.com/RRHO2/RRHO2)¹⁶.

Gene ontology and upstream regulator analysis

Gene ontology was performed in R using the *enrichR* package with our DEG lists as input. Ingenuity Pathway Analysis (IPA; Qiagen) was used to predict upstream regulators. Union heatmaps for the

regulators were generated at <https://software.broadinstitute.org/morpheus>.

Alluvial plots

Alluvial plots were generated using the R *ggalluvial* package (0.12.3)⁸⁸.

Motif enrichment analysis

We used Multiple Expectation Maximizations for Motif Elicitation (MEME) Suite for Simple Enrichment Analysis (SEA)⁹¹. Union heatmaps (<https://software.broadinstitute.org/morpheus>) highlight the top 30 motifs for behavioral conditions.

Gene co-expression network analysis

We used multiscale embedded gene co-expression network analysis (MEGENA)⁹² to construct gene modules (sunburst plots). In addition, an algorithm for the reconstruction of accurate cellular networks (ARACNE)⁹³ was used to identify likely transcriptional regulators. We used ARACNE-AP and the “MEGENA” R-package and aesthetics were modified using the R-package github.com/mw201608/sunburst.shiny⁹².

Comparisons with human RNA-seq CUD dataset

RRHO2 and heatmaps were generated to compare gene expression patterns between WD/Ext groups in rats and human CUD⁹. In brief, postmortem brain samples were obtained from subjects who died from cocaine intoxication. Rat NAc-core and NAc-shell were separately compared to whole NAc samples of CUD subjects. Significance for human DEGs was set at a fold-change (FC) of $\pm 25\%$ and nominal $p < 0.05$.

Statistics

Behavioral data were plotted as mean \pm standard error (SEM) and statistical significance was established as $p < 0.05$ using Fisher exact test, repeated measures (mixed model), two-way, or one-way ANOVAs, followed by Sidak post-hoc analysis (Prism 9). Percent change was described as ([active presses in T2 - active presses in T1] / total active presses) $\times 100$. Plots and drawings using Prism 9, biorender.com, the “tidyverse” R-package (1.3.1) and github.com/eackermann/ratpack.

Reporting summary

Further information on research design is available in the Nature Portfolio Reporting Summary linked to this article.

Data availability

The RNA-seq data generated in this study are available at the Gene Expression Omnibus (GEO) with the accession number GSE264129. Other supportive data are available as Source Data and Supplementary Information. All human information was previously reported in Mews and Cunningham et al., 2023, which is also cited throughout the present manuscript. Source data are provided with this paper.

Code availability

All used software, codes, and statistical analyses were described/provided in the methods, supplement, and throughout the manuscript. No custom software/codes were used. The DESeq2 R package (DESeq2 version 1.28.1) was used to normalize gene read counts into VST values. The MEGENA R package (MEGENA version 1.3.7) was used for all MEGENA analyses. Prior to MEGENA analysis and VST (variance Stabilizing Transformation) normalization, lowly expressed genes were eliminated, with only those genes that had a non-normalized read count of at least 6 reads in 11 samples being used as a basis for downstream analysis. For MEGENA analysis, it was desired that only the genes with the highest variation be used for network generation. Towards this end, the genes with the top 8000 highest standard deviations in the VST-normalized expression matrix were selected for use in MEGENA. MEGENA was implemented using the following parameters: (n.cores=24;

doPar=TRUE; method="pearson"; FDR.cutoff = 0.05; module.pval = 0.05; hub.pval = 0.05; cor.perm = 50; hub.perm = 100). For running ARACNE-AP, version 2016-04-01 of ARACNE-AP was implemented. VST-normalized expression of all genes was used as input for ARACNE-AP. The version of EnrichR used for ontological enrichment was version 2.1. Motif enrichment analysis was performed using the MEME suite (version 5.5.2). The promoter locations of differentially expressed genes were converted to fasta format using the bedtools (version 2.29.2) "getfasta" function. The "JASPAR2018_CORE Vertebrates non-redundant" MEME database was used as the reference database for running Simple Enrichment Analysis (SEA) on the selected promoter sequences.

References

- Koob, G. F. & Volkow, N. D. Neurocircuitry of Addiction. *Neuropsychopharmacol* **35**, 217–238 (2010).
- Myers, K. M. & Carlezon, W. A. Jr. Extinction of drug- and withdrawal-paired cues in animal models: Relevance to the treatment of addiction. *Neurosci. Biobehav. Rev.* **35**, 285–302 (2010).
- Fuchs, R. A., Lasseter, H. C., Ramirez, D. R. & Xie, X. Relapse to drug seeking following prolonged abstinence: the role of environmental stimuli. *Drug Discov. Today Dis. Models* **5**, 251–258 (2008).
- Eipper-Mains, J. E. et al. Effects of cocaine and withdrawal on the mouse nucleus accumbens transcriptome. *Genes Brain Behav.* **12**, 21–33 (2013).
- Russo, S. J. & Nestler, E. J. The brain reward circuitry in mood disorders. *Nat. Rev. Neurosci.* **14**, 609–625 (2013).
- Marchant, N. J., Campbell, E. J., Pelloux, Y., Bossert, J. M. & Shaham, Y. Context-induced relapse after extinction versus punishment: similarities and differences. *Psychopharmacology* **236**, 439–448 (2019).
- Scofield, M. D. et al. The Nucleus Accumbens: Mechanisms of Addiction across Drug Classes Reflect the Importance of Glutamate Homeostasis. *Pharm. Rev.* **68**, 816–871 (2016).
- Reichel, C. M. & Bevins, R. A. Forced abstinence model of relapse to study pharmacological treatments of substance use disorder. *Curr. Drug Abus. Rev.* **2**, 184–194 (2009).
- Mews, P. et al. Convergent abnormalities in striatal gene networks in human cocaine use disorder and mouse cocaine administration models. *Sci. Adv.* **9**, eadd8946 (2023).
- Garcia-Keller, C. et al. Relapse-Associated Transient Synaptic Potentiation Requires Integrin-Mediated Activation of Focal Adhesion Kinase and Cofilin in D1-Expressing Neurons. *J. Neurosci.* **40**, 8463–8477 (2020).
- Garcia-Keller, C. et al. Extracellular Matrix Signaling Through $\beta 3$ Integrin Mediates Cocaine Cue-Induced Transient Synaptic Plasticity and Relapse. *Biol. Psychiatry* **86**, 377–387 (2019).
- Pardo-Garcia, T. R. et al. Ventral Pallidum Is the Primary Target for Accumbens D1 Projections Driving Cocaine Seeking. *J. Neurosci.* **39**, 2041–2051 (2019).
- Scofield, M. D. et al. Gq-DREADD Selectively Initiates Glial Glutamate Release and Inhibits Cue-induced Cocaine Seeking. *Biol. Psychiatry* **78**, 441–451 (2015).
- Roberts-Wolfe, D., Bobadilla, A.-C., Heinsbroek, J. A., Neuhofer, D. & Kalivas, P. W. Drug Refraining and Seeking Potentiate Synapses on Distinct Populations of Accumbens Medium Spiny Neurons. *J. Neurosci.* **38**, 7100–7107 (2018).
- Gass, J. T. & Chandler, L. J. The Plasticity of Extinction: Contribution of the Prefrontal Cortex in Treating Addiction through Inhibitory Learning. *Front Psychiatry* **4**, 46 (2013).
- Cahill, K. M., Huo, Z., Tseng, G. C., Logan, R. W. & Seney, M. L. Improved identification of concordant and discordant gene expression signatures using an updated rank-rank hypergeometric overlap approach. *Sci. Rep.* **8**, 9588 (2018).
- Pearl, D. R., Andrade, A. K., Logan, C. N., Knackstedt, L. A. & Murray, J. E. Regulation of cocaine-related behaviours by estrogen and progesterone. *Neurosci. Biobehav. Rev.* **135**, 104584 (2022).
- Brown, A. N., Vied, C., Dennis, J. H. & Bhidé, P. G. Nucleosome Repositioning: A Novel Mechanism for Nicotine- and Cocaine-Induced Epigenetic Changes. *PLoS One* **10**, e0139103 (2015).
- Atehortua Martinez, L. A. et al. Individual differences in cocaine-induced conditioned place preference in male rats: Behavioral and transcriptomic evidence. *J. Psychopharmacol.* **36**, 1161–1175 (2022).
- Hwang, C. K. et al. Dopamine receptor regulating factor, DRRF: A zinc finger transcription factor. *Proc. Natl Acad. Sci. USA* **98**, 7558–7563 (2001).
- Chen, H., Qiang, H., Fan, K., Wang, S. & Zheng, Z. The snoRNA MBII-52 regulates cocaine-induced conditioned place preference and locomotion in mice. *PLoS One* **9**, e99986 (2014).
- Narayana, P. A. et al. Chronic cocaine administration causes extensive white matter damage in brain: diffusion tensor imaging and immunohistochemistry studies. *Psychiatry Res* **221**, 220–230 (2014).
- Vigil, F. A. & Giese, K. P. Calcium/calmodulin-dependent kinase II and memory destabilization: a new role in memory maintenance. *J. Neurochem* **147**, 12–23 (2018).
- Gentile, T. A. et al. Synthetic cathinone MDPV enhances reward function through purinergic P2X7 receptor-dependent pathway and increases P2X7 gene expression in nucleus accumbens. *Drug Alcohol Depend.* **197**, 22–27 (2019).
- Rice, J. & Gu, C. Function and Mechanism of Myelin Regulation in Alcohol Abuse and Alcoholism. *Bioessays* **41**, e1800255 (2019).
- Xu, S.-J. et al. Chromatin-mediated alternative splicing regulates cocaine-reward behavior. *Neuron* **109**, 2943–2966.e8 (2021).
- Barylko, B. et al. Palmitoylation-regulated interactions of the pseudokinase calmodulin kinase-like vesicle-associated with membranes and Arc/Arg3.1. *Front. Synaptic Neurosci.* **14**, 926570 (2022).
- Hauser, S. R. et al. The 5-HT7 receptor as a potential target for treating drug and alcohol abuse. *Front Neurosci.* **8**, 448 (2014).
- Gancarz, A. M. et al. Activin receptor signaling regulates cocaine-primed behavioral and morphological plasticity. *Nat. Neurosci.* **18**, 959–961 (2015).
- Kozlova, A. et al. Sex-specific nicotine sensitization and imprinting of self-administration in rats inform GWAS findings on human addiction phenotypes. *Neuropsychopharmacology* **46**, 1746–1756 (2021).
- Rymut, H. E. et al. Prefrontal Cortex Response to Prenatal Insult and Postnatal Opioid Exposure. *Genes (Basel)* **13**, 1371 (2022).
- lck, R. et al. Genetic overlap between mood instability and alcohol-related phenotypes suggests shared biological underpinnings. *Neuropsychopharmacology* **47**, 1883–1891 (2022).
- Berhow, M. T., Hiroi, N., Kobierski, L. A., Hyman, S. E. & Nestler, E. J. Influence of cocaine on the JAK-STAT pathway in the mesolimbic dopamine system. *J. Neurosci.* **16**, 8019–8026 (1996).
- Martínez-Sánchez, S., Aragon, C. M. G. & Salvador, A. Cocaine-induced locomotor activity is enhanced by exogenous testosterone. *Physiol. Behav.* **76**, 605–609 (2002).
- Menéndez-Delmestre, R. & Segarra, A. C. Testosterone is essential for cocaine sensitization in male rats. *Physiol. Behav.* **102**, 96–104 (2011).
- Dash, S. et al. Cocaine-regulated microRNA miR-124 controls poly (ADP-ribose) polymerase-1 expression in neuronal cells. *Sci. Rep.* **10**, 11197 (2020).
- Shaham, Y., Shalev, U., Lu, L., De Wit, H. & Stewart, J. The reinstatement model of drug relapse: history, methodology and major findings. *Psychopharmacology* **168**, 3–20 (2003).
- Kalivas, P. W., Peters, J. & Knackstedt, L. Animal models and brain circuits in drug addiction. *Mol. Inter.* **6**, 339–344 (2006).
- Maren, S., Phan, K. L. & Liberzon, I. The contextual brain: implications for fear conditioning, extinction and psychopathology. *Nat. Rev. Neurosci.* **14**, 417–428 (2013).
- Hennings, A. C., McClay, M., Lewis-Peacock, J. A. & Dunsmoor, J. E. Contextual reinstatement promotes extinction generalization in healthy adults but not PTSD. *Neuropsychologia* **147**, 107573 (2020).

41. Visser, E. et al. Extinction of Cocaine Memory Depends on a Feed-Forward Inhibition Circuit Within the Medial Prefrontal Cortex. *Biol. Psychiatry* **91**, 1029–1038 (2022).
42. Pickens, C. L. et al. Neurobiology of the incubation of drug craving. *Trends Neurosci.* **34**, 411–420 (2011).
43. Bouton, M. E., Westbrook, R. F., Corcoran, K. A. & Maren, S. Contextual and Temporal Modulation of Extinction: Behavioral and Biological Mechanisms. *Biol. Psychiatry* **60**, 352–360 (2006).
44. Furlong, T. M., Pan, M. J. & Corbit, L. H. The effects of compound stimulus extinction and inhibition of noradrenaline reuptake on the renewal of alcohol seeking. *Transl. Psychiatry* **5**, e630–e630 (2015).
45. Wiggins, A. T., Pacchioni, A. M. & Kalivas, P. W. Integrin expression is altered after acute and chronic cocaine. *Neurosci. Lett.* **450**, 321–323 (2009).
46. Huang, Y. H., Schlüter, O. M. & Dong, Y. Cocaine-induced homeostatic regulation and dysregulation of nucleus accumbens neurons. *Behav. Brain Res* **216**, 9–18 (2011).
47. Cummings, B. S. et al. Differential effects of cocaine exposure on the abundance of phospholipid species in rat brain and blood. *Drug Alcohol Depend.* **152**, 147–156 (2015).
48. Lin, Y. et al. Cocaine modifies brain lipidome in mice. *Mol. Cell. Neurosci.* **85**, 29–44 (2017).
49. Wang, J. et al. Cascades of Homeostatic Dysregulation Promote Incubation of Cocaine Craving. *J. Neurosci.* **38**, 4316–4328 (2018).
50. Campbell, R. R. et al. Cocaine induces paradigm-specific changes to the transcriptome within the ventral tegmental area. *Neuropsychopharmacol* **46**, 1768–1779 (2021).
51. Teague, C. D. & Nestler, E. J. Key transcription factors mediating cocaine-induced plasticity in the nucleus accumbens. *Mol. Psychiatry* **27**, 687–709 (2022).
52. Nestler, E. J., Barrot, M. & Self, D. W. Δ FosB: A sustained molecular switch for addiction. *Proc. Natl Acad. Sci. USA* **98**, 11042–11046 (2001).
53. Bossert, J. M., Poles, G. C., Wihbey, K. A., Koya, E. & Shaham, Y. Differential effects of blockade of dopamine D1-family receptors in nucleus accumbens core or shell on reinstatement of heroin seeking induced by contextual and discrete cues. *J. Neurosci.* **27**, 12655–12663 (2007).
54. Martínez-Rivera, F. J. et al. Neuroplasticity transcript profile of the ventral striatum in the extinction of opioid-induced conditioned place preference. *Neurobiol. Learn Mem.* **163**, 107031 (2019).
55. Bilodeau, J. & Schwendt, M. Post-cocaine changes in regulator of G-protein signaling (RGS) proteins in the dorsal striatum: Relevance for cocaine-seeking and protein kinase C-mediated phosphorylation. *Synapse* **70**, 432–440 (2016).
56. Zhang, Y. et al. Transcriptomics of Environmental Enrichment Reveals a Role for Retinoic Acid Signaling in Addiction. *Front Mol. Neurosci.* **9**, 119 (2016).
57. Bagley, J. R. et al. Estradiol increases choice of cocaine over food in male rats. *Physiol. Behav.* **203**, 18–24 (2019).
58. Krishnan, V. et al. Molecular adaptations underlying susceptibility and resistance to social defeat in brain reward regions. *Cell* **131**, 391–404 (2007).
59. Di Chiara, G. Nucleus accumbens shell and core dopamine: differential role in behavior and addiction. *Behavioural Brain Res.* **137**, 75–114 (2002).
60. Peters, J., Kalivas, P. W. & Quirk, G. J. Extinction circuits for fear and addiction overlap in prefrontal cortex. *Learn Mem.* **16**, 279–288 (2009).
61. Peters, J., Dieppa-Perea, L. M., Melendez, L. M. & Quirk, G. J. Induction of fear extinction with hippocampal-infralimbic BDNF. *Science* **328**, 1288–1290 (2010).
62. Barker, J. M., Taylor, J. R., De Vries, T. J. & Peters, J. Brain-derived neurotrophic factor and addiction: Pathological versus therapeutic effects on drug seeking. *Brain Res* **1628**, 68–81 (2015).
63. Autry, A. E. & Monteggia, L. M. Brain-derived neurotrophic factor and neuropsychiatric disorders. *Pharm. Rev.* **64**, 238–258 (2012).
64. McGinty, J. F. BDNF as a therapeutic candidate for cocaine use disorders. *Addiction Neurosci.* **2**, 100006 (2022).
65. Kaushal, J. B. et al. The regulation of Hh/Gli1 signaling cascade involves Gsk3 β -mediated mechanism in estrogen-derived endometrial hyperplasia. *Sci. Rep.* **7**, 6557 (2017).
66. Sun, Y. et al. Estrogen promotes stemness and invasiveness of ER-positive breast cancer cells through Gli1 activation. *Mol. Cancer* **13**, 137 (2014).
67. Wang, Y. et al. The crosstalk of mTOR/S6K1 and Hedgehog pathways. *Cancer Cell* **21**, 374–387 (2012).
68. Li, H.-C. et al. mTOR regulates cocaine-induced behavioural sensitization through the SynDIG1-GluA2 interaction in the nucleus accumbens. *Acta Pharm. Sin.* **43**, 295–306 (2022).
69. Pan, Y. et al. The role of Twist1 in mutant huntingtin-induced transcriptional alterations and neurotoxicity. *J. Biol. Chem.* **293**, 11850–11866 (2018).
70. McClung, C. A. & Nestler, E. J. Neuroplasticity Mediated by Altered Gene Expression. *Neuropsychopharmacol* **33**, 3–17 (2008).
71. Robison, A. J. & Nestler, E. J. Transcriptional and epigenetic mechanisms of addiction. *Nat. Rev. Neurosci.* **12**, 623–637 (2011).
72. Bingor, A., Azriel, M., Amiad, L. & Yaka, R. Potentiated Response of ERK/MAPK Signaling is Associated with Prolonged Withdrawal from Cocaine Behavioral Sensitization. *J. Mol. Neurosci.* **71**, 2229–2236 (2021).
73. Kokane, S. S. & Perrotti, L. I. Sex Differences and the Role of Estradiol in Mesolimbic Reward Circuits and Vulnerability to Cocaine and Opiate Addiction. *Front Behav. Neurosci.* **14**, 74 (2020).
74. Jarvis, R. et al. Cocaine Self-administration and Extinction Inversely Alter Neuron to Glia Exosomal Dynamics in the Nucleus Accumbens. *Front Cell Neurosci.* **13**, 581 (2019).
75. NIDA. Principles of Drug Addiction Treatment: A Research-Based Guide: Third Edition. (2018).
76. Savell, K. E. et al. A dopamine-induced gene expression signature regulates neuronal function and cocaine response. *Sci. Adv.* **6**, eaba4221 (2020).
77. Campbell, R. R. & Lobo, M. K. Neurobiological mechanisms underlying psychostimulant use. *Curr. Opin. Neurobiol.* **83**, 102786 (2023).
78. Calipari, E. S. et al. Synaptic Microtubule-Associated Protein EB3 and SRC Phosphorylation Mediate Structural and Behavioral Adaptations During Withdrawal From Cocaine Self-Administration. *J. Neurosci.* **39**, 5634–5646 (2019).
79. Paxinos, G. & Watson, C. *The Rat Brain in Stereotaxic Coordinates*. (Elsevier, Amsterdam, 2007).
80. Cullinan, W. E., Herman, J. P., Battaglia, D. F., Akil, H. & Watson, S. J. Pattern and time course of immediate early gene expression in rat brain following acute stress. *Neuroscience* **64**, 477–505 (1995).
81. Perrin-Terrin, A.-S. et al. The c-FOS Protein Immunohistological Detection: A Useful Tool As a Marker of Central Pathways Involved in Specific Physiological Responses In Vivo and Ex Vivo. *J. Vis. Exp.* 53613 <https://doi.org/10.3791/53613> (2016).
82. Lu, L., Koya, E., Zhai, H., Hope, B. T. & Shaham, Y. Role of ERK in cocaine addiction. *Trends Neurosci.* **29**, 695–703 (2006).
83. Bahrami, S. & Drabløs, F. Gene regulation in the immediate-early response process. *Adv. Biol. Regul.* **62**, 37–49 (2016).
84. Yeh, S.-Y. et al. Cell Type-Specific Whole-Genome Landscape of Δ FOSB Binding in the Nucleus Accumbens After Chronic Cocaine Exposure. *Biol. Psychiatry* **94**, 367–377 (2023).
85. Holt, L. M. et al. Astrocytic CREB in nucleus accumbens promotes susceptibility to chronic stress. *bioRxiv* 2024.01.15.575728 <https://doi.org/10.1101/2024.01.15.575728> (2024).
86. Walker, D. M. et al. Cocaine Self-administration Alters Transcriptome-wide Responses in the Brain's Reward Circuitry. *Biol. Psychiatry* **84**, 867–880 (2018).

87. Walker, D. M., Cunningham, A. M. & Nestler, E. J. Reply to: Multiple Comparisons and Inappropriate Statistical Testing Lead to Spurious Sex Differences in Gene Expression. *Biol. Psychiatry* **91**, e3–e5 (2022).
88. Browne, C. J. et al. Transcriptional signatures of heroin intake and relapse throughout the brain reward circuitry in male mice. *Sci. Adv.* **9**, eadg8558 (2023).
89. McKenzie, A. T. et al. Brain Cell Type Specific Gene Expression and Co-expression Network Architectures. *Sci. Rep.* **8**, 8868 (2018).
90. Pérez-Silva, J. G., Araujo-Voces, M. & Quesada, V. nVenn: generalized, quasi-proportional Venn and Euler diagrams. *Bioinformatics* **34**, 2322–2324 (2018).
91. Bailey, T. L., Johnson, J., Grant, C. E. & Noble, W. S. The MEME Suite. *Nucleic Acids Res* **43**, W39–W49 (2015).
92. Song, W.-M. & Zhang, B. Multiscale Embedded Gene Co-expression Network Analysis. *PLoS Comput Biol.* **11**, e1004574 (2015).
93. Margolin, A. A. et al. ARACNE: An Algorithm for the Reconstruction of Gene Regulatory Networks in a Mammalian Cellular Context. *BMC Bioinforma.* **7**, S7 (2006).

Acknowledgements

This work was supported by NIH Grants: T32DA007135-33 & K01DA054306 to F.J.M.R. and T32DA053558 to L.M.H. R01DA007359 & P01DA047233 to E.J.N. R00AA027839 to P.M. and F99NS129172 to A.M.T. The authors want to thank Joseph Landry and James Callens (Yasmin Hurd Lab); and Giselle Rojas, Kyra Schmidt, Nathalia Pulido, Katherine Beach, Stephen Pirpinias, Angélica Torres-Berrio, Yun Young Yim, Clementine Blaschke, Kinneret Rosen and Ezekiell Mouzon (Nestler Lab); Perezhil Nagendrakumar (Martinez-Rivera Lab) for technical support, scientific feedback, and bioinformatic assistance. We also want to thank Drs. Paul Kenny and Yavin Shaham for their advice and scientific discussions.

Author contributions

F.J.M.R., A.M.T., L.M.H. and E.J.N. designed the original study/idea. F.J.M.R., A.M.T. and S.T. performed the behavioral experiments and surgeries. F.J.M.R., A.M.T., S.T. and R.F., collected brain samples. F.J.M.R., S.T., L.M.H. and S.Y.Y., processed the tissue for RNA preparation, library preparation and quality control. M.E., L.M.H., C.J.B., F.J.M.R., P.M. and L.S. performed and/or were involved in bioinformatic analyses. F.J.M.R., L.M.H. and E.J.N. wrote the initial manuscript. E.J.N. supervised the project. All authors discussed the results and commented on and edited the final version of the manuscript.

Competing interests

The authors declare no competing interests.

Additional information

Supplementary information The online version contains supplementary material available at <https://doi.org/10.1038/s41467-025-58151-4>.

Correspondence and requests for materials should be addressed to Freddyson J. Martínez-Rivera, Leanne M. Holt or Eric J. Nestler.

Peer review information *Nature Communications* thanks Marcelo Wood and the other, anonymous, reviewer(s) for their contribution to the peer review of this work. A peer review file is available.

Reprints and permissions information is available at <http://www.nature.com/reprints>

Publisher's note Springer Nature remains neutral with regard to jurisdictional claims in published maps and institutional affiliations.

Open Access This article is licensed under a Creative Commons Attribution-NonCommercial-NoDerivatives 4.0 International License, which permits any non-commercial use, sharing, distribution and reproduction in any medium or format, as long as you give appropriate credit to the original author(s) and the source, provide a link to the Creative Commons licence, and indicate if you modified the licensed material. You do not have permission under this licence to share adapted material derived from this article or parts of it. The images or other third party material in this article are included in the article's Creative Commons licence, unless indicated otherwise in a credit line to the material. If material is not included in the article's Creative Commons licence and your intended use is not permitted by statutory regulation or exceeds the permitted use, you will need to obtain permission directly from the copyright holder. To view a copy of this licence, visit <http://creativecommons.org/licenses/by-nc-nd/4.0/>.

© The Author(s) 2025